Motion Analysis for Decentralized Control of N-Module Hyper-Redundant Manipulators

Timothy Vittor
Richard Willgoss
Mechatronics Research Group
UNSW, Sydney 2052, Australia
timothy.vittor@student.unsw.edu.au
r.willgoss@unsw.edu.au

Abstract

Effective manipulators are often constructed modularly and the benefits of breaking away from centralised control are being actively explored. Previously, we reported a stability analysis that can form the basis of a general analysis of hyper-redundant manipulators utilising decentralised control. A two-link, single degree of freedom system was explicated. We now report an extension of the stability analysis to an n-module single degree of freedom system. This paper redefines the bounds of stable control by showing that classical stability is only required for two roots from the characteristic equation for an unique goal to be found. The remaining roots can be unstable in traversing to the goal but settle at a marginal stability point when the goal is reached. This property is a reflection of the independance given to each module in seeking the goal and is different to an analysis of centralised control scenarios.

1 Introduction

Redundancy in Manipulators introduces flexibility in hardware reducing a manipulator's task-specific application requirements. Manipulators can become more effective in negotiating unmapped environments when they can use redundancy to navigate with a sensible motion in unpredictable surroundings. Applications that benefit from the motion of such manipulators can be as diverse as moving inside nuclear reactors [Mclean and Cameron, 2003; William II and Mayhew IV, 1997; Marzwell and Slifko, 1995; Mavroidas, *et al.*, 1995] to movement in amongst trees to pick fruits in automated harvesting [Sarig, 1993; Hayashi, *et al.*, 2002; Henton, *et al.*, 2002].

The shift to flexible redundant hardware configurations has become feasible with the implementation of rapidly deployable manipulator systems [Paredis *et al.*, 1996] designed and constructed as Reconfigurable Modular Manipulators (RMM). RMM systems are also capable of developing their own inverse kinematics using real time algorithms [Kelmar and Khosia, 1990; Schmitz, *et al.*, 1989; Kelmar and Khosia, 1988] once a system configuration is decided upon. However, the use of multiple processors, working in a modular framework, but still communicating with a central processor, presents real-time co-ordination problems [Yamakita, *et al.*, 2003; Matsuno and Suenaga, 2003] constraining system controllability. For increased redundancy, the modeling and design procedures lead to more complex algorithms that increase computational delays, again complicating the system's controllability.

Centrally controlled system, without further constraints or heuristics, cannot create determinate actions of redundant manipulators, since there are multiple infinities of solutions that can achieve a given goal and no way of discriminating between them. This has led to determining optimal paths whereby multiple solutions are revised with the anticipation of finding a single path satisfying say a cost-benefit function [Chernousko, *et al.*, 1994]. There are currently two preferred means of controlling redundant manipulators. Firstly, the constraints on motion are calculated dynamically during motion [Baillieul, 1985]. Secondly, heuristic constraints are put upon each degree of freedom [Liegeois, 1977]. Research in this field has largely focused on offline control requiring significant path planning time and a known static environment for negotiating obstacles [Ahuactzin and Gupta, 1995; Zlajpah and Nemec, 2002; Kohout, 2000].

To control redundant reconfigurable systems, it has been found that decentralized control architectures are desirable [Yook, *et al.*, 1997] because they distribute decision making into simpler and faster components. Researchers in multi-robot systems with shared information and control are currently addressing such issues, investigating behaviors to flock, disperse, aggregate, forage, collectively explore environments and follow trails reviewed in [Winfield, 2000; Shen, *et al.*, 2002; Kamimura, 2003; Arai, *et al.*, 2002]. Research in this field is developing fast and has the interest of both the military and emergency services [Jantapremjit and Austin, 2001; Unmanned Systems, 2005].

In this paper, the stability and solution space of of the Modular Decentralised Control (MDC) approach [Vittor, *et al.*, 2003; Vittor, *et al.*, 2004] is investigated in order to predict end effector motion for an n-module hyper-redundant manipulator. The approach utilizes a physical modular link layout of a redundant manipulator allowing multiple link-embedded processors to work to achieve a common goal. This approach has already enabled full control of redundancy, use of an arbitrary number of modules and fascilitated incremental

degradation in that a system will still achieve a common goal even when modules fail and are not replaced.

Section 2 gives a brief review of the MDC approach and what is meant by stability. Sections 3 provides an extension of state space analysis to three or more module manipulators. Section 4 provides numerical examples demonstrating the stability and solution space analysis of n-module manipulators using the MDC approach.

2 Modular Decentralised Control

The MDC method for RMM systems utilizes the concept of modular manipulators connected together to allow multiple module-embedded processors to work to achieve a common goal. Each module is independent in control actions and can individually respond to the immediate surroundings.

An iconic manipulator control was created out of a generic module type, 100mm in length. Each module used here was, in a separate exercise [Vittor, *et al.*, 2003], designed to give two-degrees of freedom manipulation. Hence with two modules, redundancy was possible although hyper-redundancy needed three modules or more to compose a system. Each module was given a two Degree of Freedom (DOF) rotational capability over ±180°. A particular configuration of an n-link manipulator is shown in Figure 2.

When the goal is recognized by the end effector's stereo vision and it's relative position becomes known, each module's prime objective is to move the common point, namely the end effecter, to that goal. As each link interprets the error independently, that module then provides actuator motions to reduce its own rotational errors to zero. In the analysis that follows, we have used one degree of freedom in each module to aid in understanding the subsequent analysis of stability. Extensions to using both degrees of freedom are also being investigated.

Previous work [Vittor and Willgoss, 2005] has shown the stability analysis for motion of a simple MDC-RMM two-module system. The regions of instability and/or oscillations as understood in classical control were found to take the form of helical toroid boundaries on one degree of freedom that are both cyclic and express complete limits for the manipulator. A modified root locus technique was used to describe how the system's stability, expressed in classical terms, changes as a function of path traversed brought about by the pseudo-independent actions of each module. Results showed a system that was ultimately stable. In addition, each root locus referred to the way the eigenvalues changed when an attempt to reach the goal took place. The motion again, according to a classical state space analysis, was seen as unstable or oscillatory within bounded regions. However, with the modified root locus technique, we can understand that the goal can be reached by a two-module manipulator in a reasonable and possibly optimal manner.

3 Manipulator System

The previous stability analysis for a two module manipulator yielded a two by two state space system matrix [Vittor and Willgoss, 2005]. This analysis is now extended to analyse three or more modules. A linearisation technique is used, based on the formation of a Jacobian relating all angular movements.

Figure 3 shows a configuration in which a goal is to be reached by n modules pseudo-independently of each other and relies on the interpretation of error from the viewpoint of each module alone. As mentioned previously in this analysis, one module now has one rotational degree of freedom associated with it.

A proportional discrete error equation is first generated where $\bar{\theta}'$, the next iteration of $\bar{\theta}$, is determined though a standard function including $\bar{\theta}$, a difference vector, $\underline{R}\left(\bar{\theta},{}^{0}\theta_{g}\right)$ and a time interval period ΔT.

$$\bar{\theta}' = \bar{\theta} + \underline{R}\left(\bar{\theta},{}^{0}\theta_{g}\right)\cdot\Delta T \qquad (1)$$

The error vector $\underline{R}\left(\bar{\theta},{}^{0}\theta_{g}\right)$ is defined in equation (2).

$$\underline{R}\left(\bar{\theta},{}^{0}\theta_{g}\right) = \begin{bmatrix} {}^{1}\theta_{g} - {}^{1}\theta_{e} \\ \vdots \\ {}^{n}\theta_{g} - {}^{n}\theta_{e} \end{bmatrix} \cdot r \qquad (2)$$

r is a scaling factor. In this first instance, we have adopted purely proportional control for simplicity. Extensions to all other variants can be included later.

${}^{i}\theta_{g}$ and ${}^{i}\theta_{e}$ are the goal and end effector positions as seen respectively in module *i* frame of

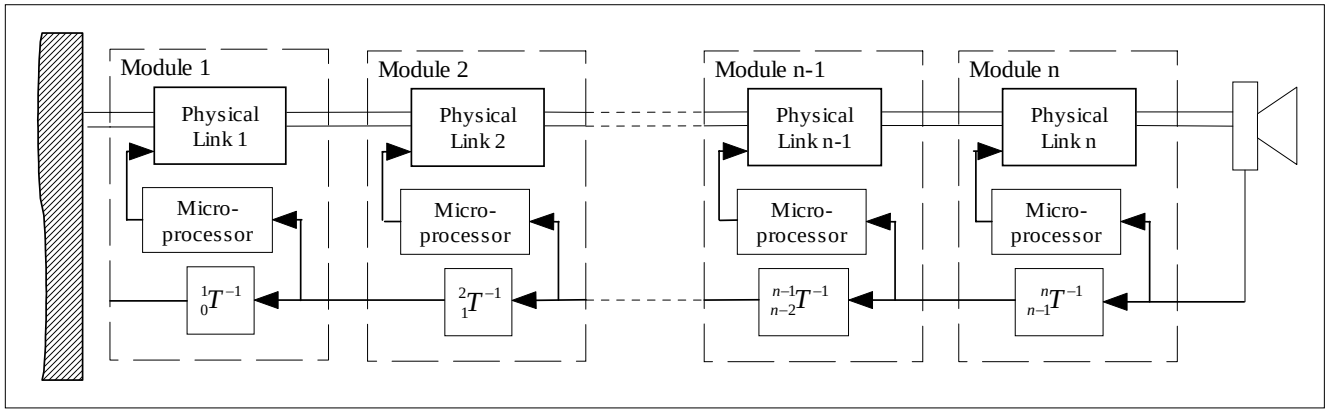

Figure 2: An n-link manipulator composed of n modules

reference. The goal in the base frame of reference is defined as $\left({}^0x_g, {}^0y_g\right)$ and is determined through a forward transformation of the goal from the end effector's frame of reference.

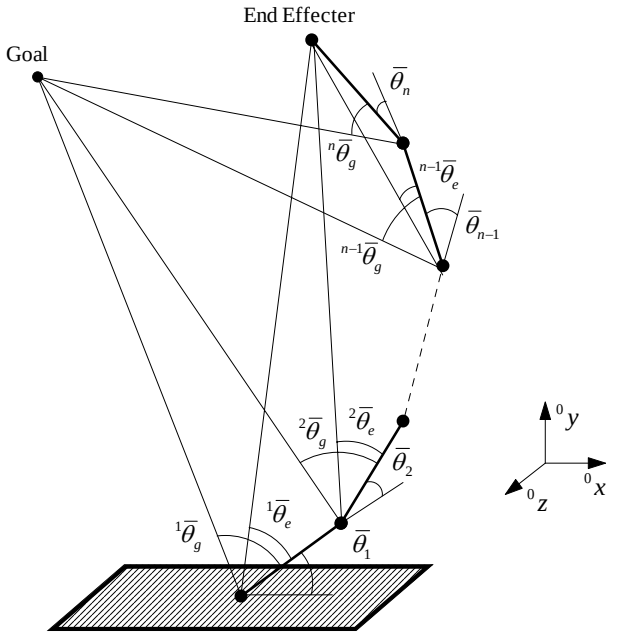

Figure 3: An n-link common goal configuration

Substituting in for the three module error vector, the main discrete equations of motion are:

$$\theta_1' = \theta_1 + \left(-\theta_1 + {}^0\theta_d - \tan^{-1}\left(\frac{l_3 S_{23} + l_2 S_2}{l_3 C_{23} + l_2 C_2 + l_1} \right) \right) \cdot r \cdot \Delta T \quad (3)$$

$$\theta_2' = \theta_2 + \left(\tan^{-1}\left(\frac{C_{12} \cdot {}^0y_g - S_{12} \cdot {}^0x_g + l_1 S_2}{C_{12} \cdot {}^0x_g + S_{12} \cdot {}^0y_g - l_1 C_2} \right) - \tan^{-1}\left(\frac{l_3 S_3}{l_3 C_3 + l_2} \right) \right) \cdot r \cdot \Delta T \quad (4)$$

$$\theta_3' = \theta_3 + \left(\tan^{-1}\left(\frac{C_{123} \cdot {}^0y_g - S_{123} \cdot {}^0x_g + l_1 S_{23} + l_2 S_3}{C_{123} \cdot {}^0x_g + S_{123} \cdot {}^0y_g - l_1 C_{23} - l_2 C_3} \right) \right) \cdot r \cdot \Delta T \quad (5)$$

Equations 3 to 5 are now made continuous via equation 6 where $\Delta T \to 0$.

$$\dot{\bar{\theta}} = \frac{\bar{\theta}' - \bar{\theta}}{\Delta T} = \left(\bar{\theta}_g - \bar{\theta}_e \right) \cdot r \quad (6)$$

Linearization, using the first terms of the Taylor series and a normalized error gain r =1 being the same in each DOF, generates a state space equation 7 for the manipulator:

$$\dot{\bar{\theta}} = \underline{A} \cdot \bar{\theta} + \underline{B} \cdot \bar{u} \quad (7)$$

where:

$$\bar{\theta} = \begin{bmatrix} \theta_1 \\ \theta_2 \\ \theta_3 \end{bmatrix}, \qquad \bar{u} = \begin{bmatrix} {}^0\theta_g \\ 0 \\ 1 \end{bmatrix}$$

The system matrix A and input B matrix in equation 8 have to be re-calculated iteratively during the motion of the manipulator as it moves towards the goal.

$$\begin{bmatrix} \dot{\theta}_1 \\ \dot{\theta}_2 \\ \dot{\theta}_3 \end{bmatrix} = \begin{bmatrix} -1 & a_{12} & a_{13} \\ a_{21} & -1 & a_{23} \\ a_{31} & a_{32} & -1 \end{bmatrix} \cdot \begin{bmatrix} \theta_1 \\ \theta_2 \\ \theta_3 \end{bmatrix} + \begin{bmatrix} 1 & 0 & b_{13} \\ 0 & 0 & b_{23} \\ 0 & 0 & b_{33} \end{bmatrix} \cdot \begin{bmatrix} {}^0\theta_g \\ 0 \\ 1 \end{bmatrix} \quad (8)$$

The coefficients are listed in the Appendix. The eigenvalues and eigenvectors are then obtained from the A matrix.

The analysis shown here can also be conducted for an n-module system, in which case, the A matrix can be analysed to obtain n eigenvalues and n eigenvectors. It is seen that, as the number of degees of freedom increases, the complexity of the analysis could become intractable, but nevertheless assessable for the n-module case by a process of induction.

4 Manipulator Solution Space Analysis

A map of the solution space for a two-module manipulator is first made before extending to three and finally n-modules. The end effector goal is positioned anywhere in the workspace where the theoretical module angles range over $\pm\pi$ radians. The motion and final solution of a manipulator is dependent on both the goal position and on the initial manipulator configuration.

4.1 Two-Module Configurations

In moving towards any goal, the unstable equilibrium points for the two-module work envelope form a square structure, as shown in Figure 4, with nine unstable equilibrium points. These points translate horizontally as a funtion of the angle to the goal in the base frame of reference ${}^0\theta_g$.

The unstable equilibrium configurations are shown in Figure 5 with corresponding numbers listed. In centralized control, they constitute singularities. In decentralized control, these points are avoided unless the unstable equilibrium point is the initial configuration of the manipulator. Theoretically, if the initial configuration lies on one of these unstable equilibrium points it will not be possible to reach the goal. However, and practically speaking any slight variation in the initial configuration will enable the manipulator to then move towards the goal.

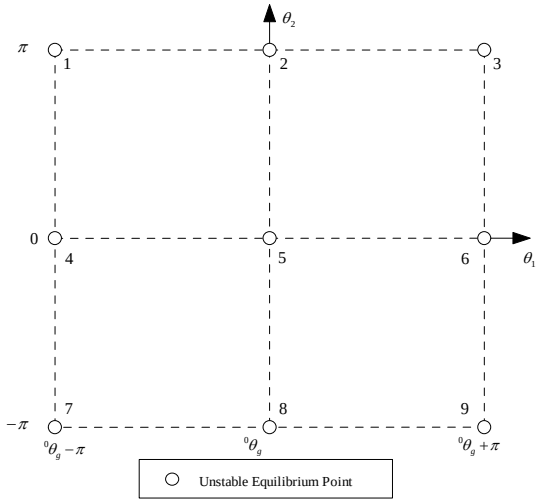

Figure 4. Two-Module Unstable Equilibrium Points

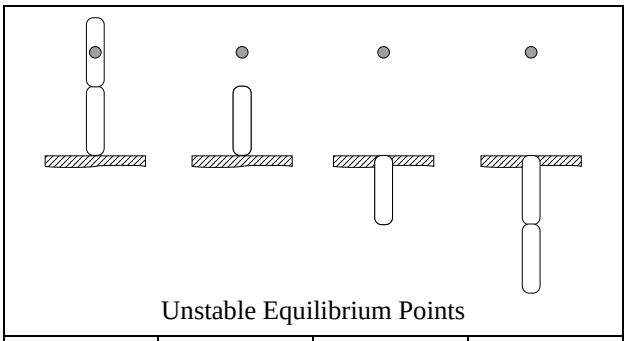

Unstable Equilibrium Points			
5	2,8	1,3,7,9	4,6

Figure 5. Two-Module Unstable Equilibrium Configurations

For a particular end effector goal position to be reached (excluding the base of the manipulator where the first module angle is arbitrary), there exist up to two distinct solution configurations for the manipulator. Varying the distance to goal from the base of the manipulator $\sqrt{{}^0x_g^2+{}^0y_g^2}$ alters the stability characterisitcs of the manipulator's motion to the goal. Previous work [Vittor and Willgoss, 2005] has found that for a two-module manipulator, three types of end effector trajectory can be found using the eigenvalues of the linearised system matrix.

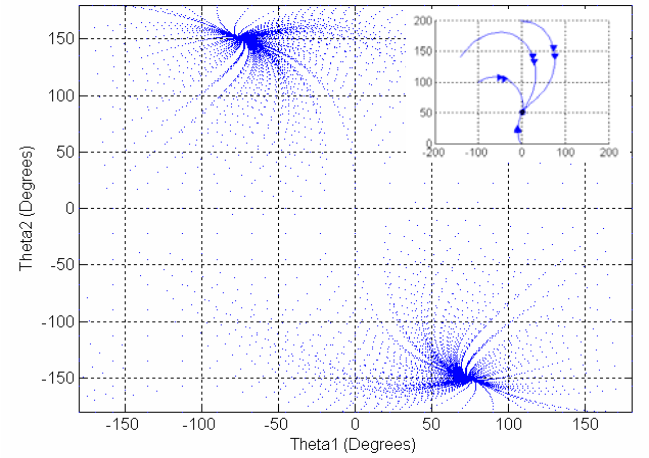

Figure 6. Two-Module Movement to a Goal at (0,50)

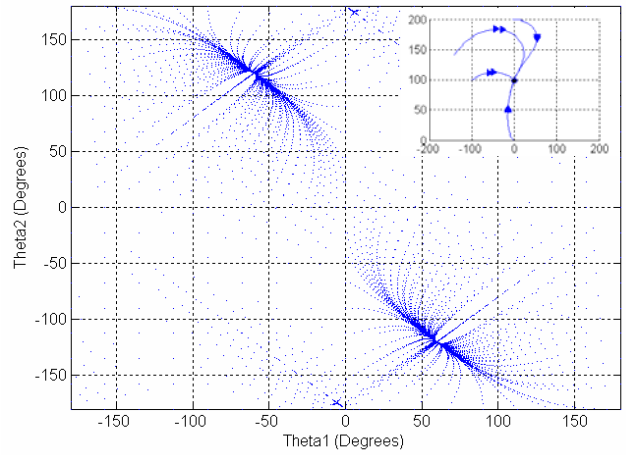

Figure 7. Two-Module Movement to a Goal at (0,100)

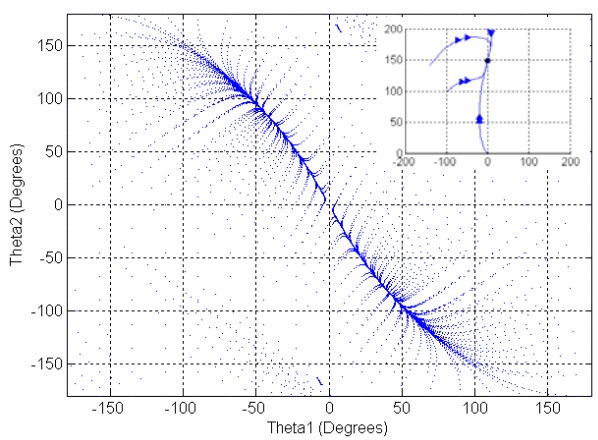

Figure 8. Two-Module Movement to a Goal at (0,150)

The three approaches to the goal are observed as shown in Figures 6 to 8. The subplots show the trajectory of the end effector to the goal from four arbitrary initial configurations. During these motions, there are instances where oscillatory and unstable behaviour in classical terms exists. However it was noted that, when the goal was reached, both eigenvalues were found to be real and stable.

The approach as shown in Figure 7 are now steriotyped as shown in Figure 9 where the goal is at (0,100). The unstable equilibrium points depend on the base angle to the goal where the case ${}^0\theta_g = 0$ is shown in Figure 9.

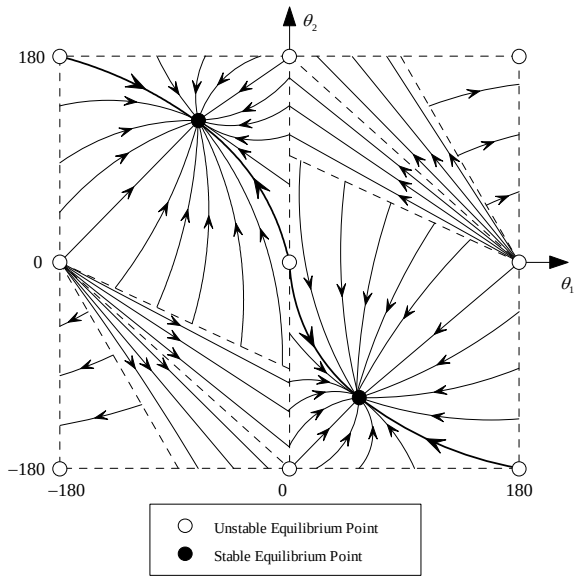

Figure 9. Two-Module Movement to a Goal at (0,100) with steriotypical approaches marked in

A special case occurs with a saddle point, indicated by numbers 2 and 8 in Figure 5. A critical line of instability occurs between points 2 and 6 and again between points 4 and 8 such that if the manipulator starts in a configuration anywhere along these lines, it will be drawn into an unstable point and theoretically stay there. Such motion is shown in Figure 10.

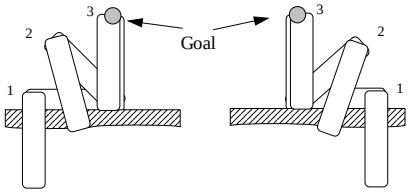

Figure 10. Saddle Point Configurations

There is also evident discontinuity in motion along the vertical vertical line $\theta_1 = {}^0\theta_g = 0$. Though motion may appear undesirable because of passing through discontinuities, such angular motions were found to result in a smooth end effector approach to the goal. The periodic motion map of the manipulator as shown in Figure 11 indicates that the pattern is extendable in both axes.

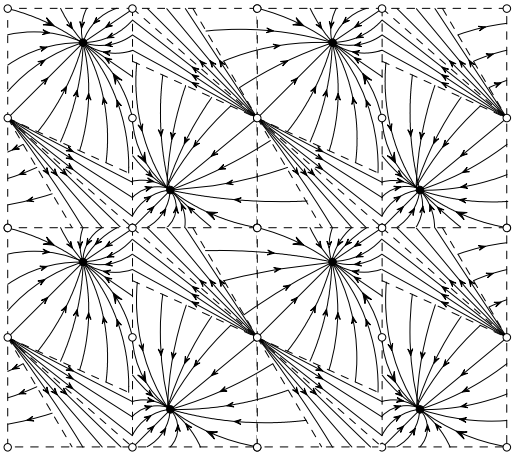

Figure 11. Periodic motion to a Goal at (0,100)

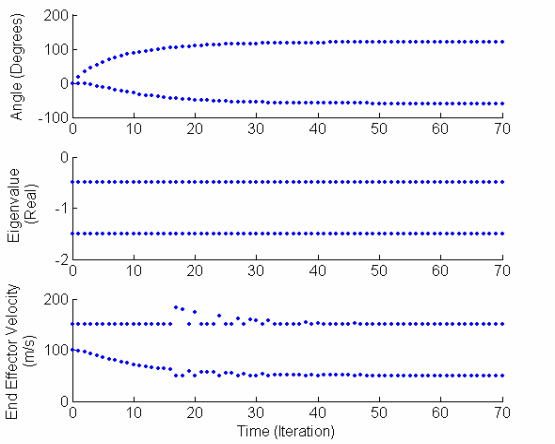

Figure 12. Motion Profile for a Two-Module Manipulator with a Goal at (0,100)

The two-system matrix eigenvectors show the module motion combinations for the manipulator that lead to end effector movement. When the eigenvectors are used into the two-module Jacobian equation 8,

$$\begin{bmatrix} {}^0\dot{x}_e \\ {}^0\dot{y}_e \end{bmatrix} = \begin{bmatrix} l_1C_1 + l_2C_{12} & l_2C_{12} \\ -l_1S_1 - l_2S_{12} & -l_2S_{12} \end{bmatrix} \cdot \begin{bmatrix} \dot{\theta}_1 \\ \dot{\theta}_2 \end{bmatrix} \quad (8)$$

the corresponding end effector trajectory can be found. The manipulator's motion, eigenvalues and corresponding end effector trajectory for an arbitrary initial configuration of the module angles $(\theta_1, \theta_2) = (-1^o, 0)$ are shown in Figure 12.

It was found that both eigenvectors resulted in contributing to end effector motion, and hence the eigenvalues both needed to be stable when the goal had been reached.

4.2 Three-Module Configurations

The previous analysis was extended to a three-module manipulator. The unstable equilibrium points within the three-module work envelope were found to form a cube structure, as shown in Figure 13 with 27 unstable equilibrium points. These points were an extension of the nine points as outlined in the two-module manipulator.

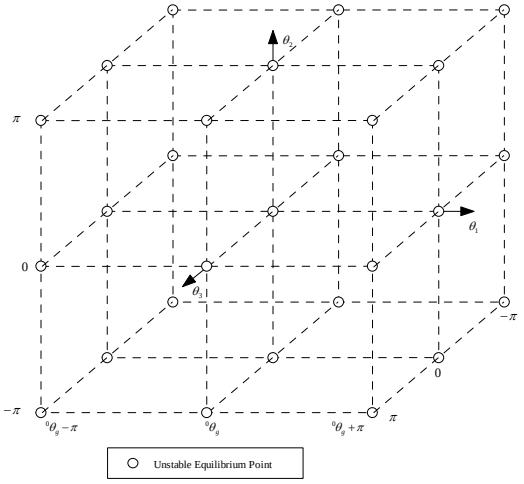

Figure 13. Three-Module Unstable Equilibrium Points

A particular solution space was found for the motion analysis of a goal at (0,100) where the lengths for the modules were all 100. An exploration of the trajectory space of the end effector resulted in discovering that the manipulator's module angle combination could settle anywhere on the 3D curve as shown in Figure 14, for the end effector goal to be successfully reached. An explanation for this property was then sought.

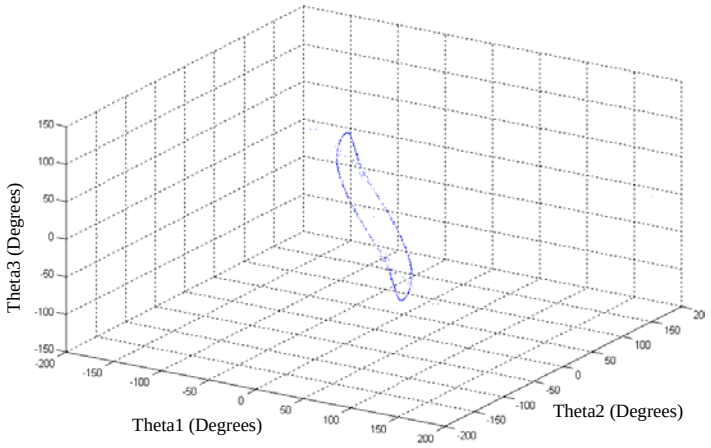

Figure 14. Three-Module Solution with a Goal at (0,100)

The three-system eigenvectors were then used in equation 9 to discover end effector trajectory movement in the same way as shown in section 4.1. The three-module Jacobian equation was found to be:

$$\begin{bmatrix} {}^0\dot{x}_e \\ {}^0\dot{y}_e \end{bmatrix} = \begin{bmatrix} l_1C_1 + l_2C_{12} + l_3C_{123} & l_2C_{12} + l_3C_{123} & l_3C_{123} \\ -l_1S_1 - l_2S_{12} - l_3S_{123} & -l_2S_{12} - l_3S_{123} & -l_3S_{123} \end{bmatrix} \cdot \begin{bmatrix} \dot{\theta}_1 \\ \dot{\theta}_2 \\ \dot{\theta}_3 \end{bmatrix} \quad (9)$$

The three-modules trajectory characteristics for an arbitrary initial configuration of the module angles $(\theta_1, \theta_2, \theta_3) = (-1^o, 0, 0)$ is shown in Figure 15.

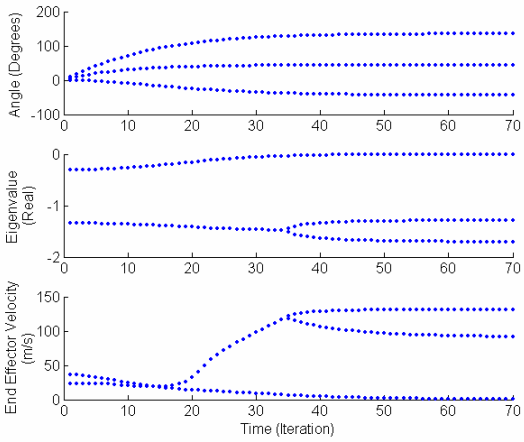

Figure 15. Motion Profile for a Three-Module Manipulator with a Goal at (0,100)

It was found that only two eignevectors resulted in giving motion to the end effector once the goal had been reached. Movement from the application of the other eigenvector enabled all three modules to change but left the end effector unmoved. This situation is an accommodation of the redundancy that existed in the manipulator. Therefore, only two eigenvalues needed to be stable for the end effector to settle on the goal. The eigenvalue corresponding to no motion in the end effector thus required only marginal stability when the goal was reached for the manipulator to settle in an unique configuration. This eigenvector was tangential to the curve at any particular solution point shown in Figure 14. Theoretically the marginal stability means the configuration of the manipulator can be moved quasi-statically without moving the end effector and remain in the new configuration without returning to the one from which it has come.

4.3 N-Module Configurations

The analysis in section 4.2 was extended to an n-module manipulator. The equilibrium points within the work envelope were found to consist of u unstable equilibrium points in an n-dimensional space where:

$$u = 3^n \quad \text{for all positive n} \quad (10)$$

Extension of the motion analysis to an n-module manipulator through corresponding n non-linear motion equations from all initial configurations in the region $-\pi \geq \theta_1, \theta_2, \cdots, \theta_{n-1}, \theta_n \geq \pi$, generates the n by n system matrix A.

$$\underline{A} = \begin{bmatrix} -1 & a_{12} & \cdots & a_{1(n-1)} & a_{1n} \\ a_{21} & -1 & & & a_{2n} \\ \vdots & & \ddots & & \vdots \\ a_{(n-1)1} & & & -1 & a_{(n-1)n} \\ a_{n1} & a_{n2} & \cdots & a_{n(n-1)} & -1 \end{bmatrix} \quad (11)$$

The motion combinations of the manipulator are observed by deriving the eigenvectors of the n-module system matrix. When the eigenvectors are used into the n-module Jacobian equation 12,

$$\begin{bmatrix} {}^0\dot{x}_e \\ {}^0\dot{y}_e \end{bmatrix} = \begin{bmatrix} j_{11} & j_{12} & \cdots & j_{1(n-1)} & j_{1n} \\ j_{21} & j_{22} & \cdots & j_{2(n-1)} & j_{2n} \end{bmatrix} \cdot \begin{bmatrix} \dot{\theta}_1 \\ \dot{\theta}_2 \\ \vdots \\ \dot{\theta}_{n-1} \\ \dot{\theta}_n \end{bmatrix} \quad (12)$$

it follows that only two eigenvectors produce motion in the end effector. With the remaining n-2 eigenvalues at marginal stability, the end effector goal is reached and the manipulator settles on one unique goal solution. This extension of eigenvector and eigenvalue analysis has been tested in MATLAB and found consistent with 1DOF module manipulators composed of up to 6 modules.

In the limit, the motion of a perfect n-module 1 DOF per module manipulator, as configured here, takes the same form as that of a plucked string with a series of oscillations taking place above a fundametal as in a Fourier frequency series.

5 Conclusions

The solution space for motion of an n-module 1 DOF per module sequencial manipulator as described in this paper has been explicated. Some motion in classical control terms could be regarded as unstable. However, upon further analysis motion to the goal is a quasi-stable trajectory.

In the simplest case, for a two-module 1 DOF system there exist two possible solution configurations for any goal. Both of these solutions constitute stable equilibrium points.

When a three-module configuration is envisiaged one eigenvector is redundant once the goal is reached in causing end effector motion. This means that only two eigenvalues need to be stable for the end effector trajectory to settle on an unique goal. The three-module solution map turns out to be a three dimensional curve in which this third eigenvector is tangential to the curve at all times.

For n-modules the remaining n-2 eigenvectors that do not make the end effector move all give rise to motion tangential to the hyper-infinity of solutions in hyper-space.

6 Future Work

In the immediate future the analysis is to be extened to 2 DOF per module in an n-module manipulator. In addition, the type of feedback which, at present is simple proportional, will be modified to include PID and other more complex scenarios.

References

[Ahuactzin and Gupta, 1995] J.M. Ahuactzin and K. Gupta, "A Motion Planning Based Approach for Inverse Kinematics of Redundant Robots: The Kinematic Roadmap" International Conference Intelligent Autonomous Systems, Karlsruhe, March 1995.

[Arai, *et al., 2002*] Tamio Arai, Enrico Pagello, and Lynne E. Parker, "Editorial: Advances in Multi-Robot Systems" IEEE Transactions on Robotics and Automation, 18(5), pp. 665-661, October, 2002.

[Baillieul, 1985] J. Baillieul, "Kinematic Programming alternatives for redundant manipulators" Proc. IEEE Int. Conf. Robotics and Automation, pp. 722-728, March, 1985.

[Chernousko, *et al.*, 1994] Felix L. Chernousko, Nikolai N. Bolotnik, and Valery G. Gradetsky, "Manipulation Robots: Dynamics, Control and Optimization" CRC Press, Florida, USA, pp.170-210, 1994.

[Hayashi, *et al.*, 2002] S. Hayashi, et al., "Robotic Harvesting System for Eggplants" JARQ 36(3), pp. 163-168, 2002.

[Henton, *et al.*, 2002] E.J. Van Henton, et al., "CUPID – An Autonomous Cucumber Picking Device" Proceedings of Mechatronics, University of Twente, June, 2002.

[Jantapremjit and Austin, 2001] P. Jantapremjit, and D. Austin, "Design of a modular Self-Reconfigurable Robot" Australian Conference on Robotics and Automation, Sydney, November, 2001.

[Kamimura, 2003] A. Kamimura, H. Kurokawa and E. Yoshida, "Automatic Locomotion Pattern Generation for Modular Robots" IEEE International Conference on Robotics and Automation, September, 2003.

[Kelmar and Khosia, 1988] L. Kelmar, and P. Khosia, "Automatic generation of kinematics for a reconfigurable modular manipulator system" Proc. IEEE Int. Conf. Robotics and Automation, Philadelphia, USA, 1988.

[Kelmar and Khosia, 1990] L. Kelmar, and P. Khosia, "Automatic generation of forward and inverse kinematics for a reconfigurable modular manipulator system" Journal of Robotics Systems Vol.7 No.4, pp. 599-619, 1990.

[Kohout, 2000] B. Kohout, "Challenges in Real-Time Obstacle Avoidance"American Association for Artificial Intelligence, 2000.

[Liegeois, 1977] A. Liegeois, "Automatic Supervisory Control of the Configuration and Behaviour of Multi-body Mechanisms", IEEE Trans. System, Man and Cybernetics, Vol. SMC-7, pp. 868-871, 1977.

[Matsuno and Suenaga, 2003] F. Matsuno and K. Suenaga, "Control of Redundant 3D Snake Robot based on Kinematic Model" IEEE International Conference on Robotics and Automation, Taipei, Taiwan, September, 2003.

[Marzwell and Slifko, 1995] N.I. Marzwell, and A. Slifko, "Visual Inspection Planar Serpentine Manipulator" NASA's Technology 2005 conference, Chicago, IL., October, 1995.

[Mavroidas, *et al.*, 1995] C.Mavroidas, P.Rowe, and S.Dubowsky, "Inferred end-point control of long reach manipulators," *Proc. IEEE/RSJ Int. Conf. Intelligent Robots and Systems* Pittsburgh, PA, pp. 71-76, Aug. 1995.

[Mclean and Cameron, 2003] A. Mclean and S. Cameron, "Path Planning and Collision Avoidance for Redundant Manipulators in 3D" IEEE International Conference on Robotics and Automation, Taipei, Taiwan, September, 2003.

[Paredis *et al.*, 1996] C.J.J. Paredis, H.B. Brown and P.K. Khosla, "A Rapidly Deployable Manipulator System" IEEE International Conference on Robotics and Automation, Minneapolis, Minnesota, April, 1996.

[Sarig, 1993] Y. Sarig, "Robotics of Fruit Harvesting: A State-of-the-art Review" Journal of Agricultural Engineering Research, 54, pp. 265-280, 1993.

[Schmitz, *et al.*, 1989] D. Schmitz, P. Khosia, R. Hoffman, and T. Kanade, "CHIMERA: A real-time programming environment for manipulator control", Proc. IEEE Int. Conf. Robotics and Automation, Vol.2, pp. 846-852, 1989.

[Shen, *et al.*, 2002] Wei-Min Shen, B. Salemi, and P. Will, "Hormone-Inspired Adaptive Communication and Distributed Control for CONRO Self-Reconfigurable Robots" IEEE Transactions on Robotics and Automation, 18(5), October, 2002.

[Unmanned Systems, 2005] Technology driven opportunities in Unmanned Systems Conference, International Quality & Productivity Centre, Canberra, Australia, September 2005.

[Vittor, *et al.*, 2003] T.Vittor, R.Willgoss and T.Furukawa, "Modular Decentralized Control of Fruit Picking Redundant Manipulator" Australian Conference on Robotics and Automation, Brisbane, December, 2003.

[Vittor, *et al.*, 2004] T.Vittor, R.Willgoss and T.Furukawa, "Hyper-Redundant Manipulator Control For Reconfigurability and Obstacle Avoidance" Australian Conference on Robotics and Automation, Canberra, December, 2004.

[Vittor and Willgoss, 2005] T.Vittor and R.Willgoss, "Stability and Motion Analysis for Decentralized Control of Modularized Manipulators", Int. Conf. Computational Intelligence, Robotics and Autonomous Systems, Singapore, December, 2005.

[William II and Mayhew IV, 1997] R.L. William II, and J.B. Mayhew IV, "Obstacle-Free Control Of The Hyper-Redundant Nasa Inspection Manipulator" Proc. of the Fifth National Conf. on Applied Mechanics and Robotics, October 12-15, 1997.

[Winfield, 2000] A. Winfield, "Distributed sensing and data collection via broken ad hoc wireless connected networks of mobile robots" In proceedings of Fifth International Symposium on Distributed Autonomous Robotic Systems, pages 273-282, 2000.

[Yamakita, *et al.*, 2003] M. Yamakita, M. Hashimoto and T. Yamada., "Control of Locomotion and Head Configuration of 3D Snake Robot (SMA)" IEEE International Conference on Robotics and Automation, September, 2003.

[Yook, *et al.*, 1997] J. Yook, D. Tilbury, K. Chervela and N. Soparkar, "Decentralized, Modular Real-Time

Control for Machining Applications" Proceedings of the American Control Conference pp 844-849.

[Zlajpah and Nemec, 2002] L. Zlajpah and B.Nemec, "Kinematic Control Algorithms for On-line Obstacle Avoidance for Redundant Manipulators" Inter. Conf. on Intelligent Robots and Systems, 2002.

Appendix

Coefficients of a three-module system A matrix.

$$a_{12} = -\frac{l_2^2 + l_3^2 + 2l_2l_3C_3 + l_1(l_3C_{23} + l_2C_2)}{l_1^2 + l_2^2 + l_3^2 + 2l_2l_3C_3 + 2l_1(l_3C_{23} + l_2C_2)}$$

$$a_{13} = -\frac{l_3^2 + l_2l_3C_3 + l_1l_3C_{23}}{l_1^2 + l_2^2 + l_3^2 + 2l_2l_3C_3 + 2l_1(l_3C_{23} + l_2C_2)}$$

$$a_{21} = \frac{-{}^0x_g{}^2 - {}^0y_g{}^2 + l_1({}^0y_gS_{10} + {}^0x_gC_{10})}{{}^0x_g{}^2 + {}^0y_g{}^2 + l_1{}^2 - 2l_1({}^0y_gS_{10} + {}^0x_gC_{10})}$$

$$a_{23} = -\frac{l_3{}^2 + l_2l_3C_{30}}{l_2{}^2 + l_3{}^2 + 2l_2l_3C_{30}}$$

$$a_{31} = \frac{-{}^0y_g^2 - {}^0x_g^2 + {}^0y_g(l_1S_1 + l_2S_{12}) + {}^0x_g(l_1C_1 + l_2C_{12})}{{}^0x_g^2 + {}^0y_g^2 + l_1^2 + l_2^2 - 2{}^0x_g(l_1C_1 + l_2C_{12}) - 2{}^0y_g(l_1S_1 \cdot + l_2S_{12}) + 2l_1l_2C_2}$$

$$a_{32} = \frac{-{}^0x_g^2 - {}^0y_g^2 - l_1^2 + {}^0x_g(2l_1C_1 + l_2C_{12}) + {}^0y_g(2l_1S_1 + l_2S_{12}) - l_1l_2C_2}{{}^0x_g^2 + {}^0y_g^2 + l_1^2 + l_2^2 - 2{}^0x_g(l_1C_1 + l_2C_{12}) - 2{}^0y_g(l_1S_1 \cdot + l_2S_{12}) + 2l_1l_2C_2}$$

$$b_{13} = \frac{l_2^2 + l_3^2 + 2l_2l_3C_3 + l_1(l_3C_{23} + l_2C_2)}{l_1^2 + l_2^2 + l_3^2 + 2l_2l_3C_3 + 2l_1(l_3C_{23} + l_2C_2)}\theta_{20} \cdots$$

$$+ \frac{l_3^2 + l_2l_3C_3 + l_1l_3C_{23}}{l_1^2 + l_2^2 + l_3^2 + 2l_2l_3C_3 + 2l_1(l_3C_{23} + l_2C_2)}\theta_{30} - \tan^{-1}\left(\frac{l_3S_{2030} + l_2S_{20}}{l_3C_{2030} + l_2C_{20} + l_1}\right)$$

$$b_{23} = -\frac{-{}^0x_g{}^2 - {}^0y_g{}^2 + l_1({}^0y_gS_{10} + {}^0x_gC_{10})}{{}^0x_g{}^2 + {}^0y_g{}^2 + l_1{}^2 - 2l_1({}^0y_gS_{10} + {}^0x_gC_{10})}\theta_{10} \cdots$$
$$+ \theta_{20} + \frac{l_3{}^2 + l_2l_3C_{30}}{l_2{}^2 + l_3{}^2 + 2l_2l_3C_{30}}\theta_{30} - \tan^{-1}\left(\frac{l_3S_{30}}{l_3C_{30} + l_2}\right)$$

$$b_{33} = -\frac{-{}^0y_g^2 - {}^0x_g^2 + {}^0y_g(l_1S_1 + l_2S_{12}) + {}^0x_g(l_1C_1 + l_2C_{12})}{{}^0x_g^2 + {}^0y_g^2 + l_1^2 + l_2^2 - 2{}^0x_g(l_1C_1 + l_2C_{12}) - 2{}^0y_g(l_1S_1 \cdot + l_2S_{12}) + 2l_1l_2C_2}\theta_{10} \cdots$$

$$- \frac{-{}^0x_g^2 - {}^0y_g^2 - l_1^2 + {}^0x_g(2l_1C_1 + l_2C_{12}) + {}^0y_g(2l_1S_1 + l_2S_{12}) - l_1l_2C_2}{{}^0x_g^2 + {}^0y_g^2 + l_1^2 + l_2^2 - 2{}^0x_g(l_1C_1 + l_2C_{12}) - 2{}^0y_g(l_1S_1 \cdot + l_2S_{12}) + 2l_1l_2C_2}\theta_{20} \cdots$$

$$+ \theta_{30} + \tan^{-1}\left(\frac{C_{102030} \cdot {}^0y_g - S_{102030} \cdot {}^0x_g + l_1S_{2030} + l_2S_{30}}{C_{102030} \cdot {}^0x_g + S_{102030} \cdot {}^0y_g - l_1C_{2030} - l_2C_{30}}\right)$$